Available online at www.sciencedirect.com
SCIENCE DIRECT®
Atmospheric Environment 39 (2005) 7276–7284
ATMOSPHERIC ENVIRONMENT
www.elsevier.com/locate/atmosenv

Saharan dust outbreak over southeastern Spain as detected by sun photometer

H. Lyamani, F.J. Olmo, L. Alados-Arboledas*

Departamento de Física Aplicada, Facultad de Ciencias, Universidad de Granada, Fuentenueva s/n.18071, Granada, Spain

Received 30 April 2005; received in revised form 8 August 2005; accepted 2 September 2005

Abstract

Characterization of mineral aerosol properties in southeastern Spain is important due to its proximity to the African continent that permit studying the Saharan dust just entering European continent before its possible mixing with anthropogenic emissions in Europe. Two Saharan dust events that occurred during 30 August–3 September and on 10 September 1998 were observed at an inland location on the outskirts of Granada in southeastern Spain. Detailed analyses including back trajectories and TOMS aerosol index maps showed transport of Saharan dust from the Sahara desert and North Africa to the study area. The dust episodes were associated with marked increases in aerosol optical depth (δ_a) at all wavelengths examined in this study. Thus δ_a (500 nm) increased from a value of ~0.2 corresponding to normal conditions up to 0.6 in the first event and up to 0.55 in the second. At the end of these events, the arrival of air masses from the Atlantic caused a sharp decrease in δ_a (500 nm) that reaches values close to those obtained before the event (~0.2). The Angström exponent α reached a minimum of 0.36 in the first event and 0.37 in the second. The Angström exponent α and aerosol optical depth values during dust events agree well with those obtained under the same kind of events in AERONET and SKYNET sites, as well as with the results obtained in ACE-2 and ACE-Asia experiments. The aerosol size distributions, retrieved from aerosol optical depth using King's method, demonstrated how the large size fraction of aerosol associated with Saharan dust dominated during these events. When Saharan dust was present, the retrieved aerosol size distributions were bimodal with a well-defined mode centred at a radius of 0.6 μm, and showed an evident increase in the large particles mode with radii in the range 0.4–2 μm. The small particle concentration during the two events did not present any marked change, and was similar to those observed on days without Saharan dust. Large particle concentration was higher by a factor of 8 than during normal conditions.

Keywords: Aerosol properties; Sun photometry; Angström parameter; Saharan dust

1. Introduction

Dust particles reflect and absorb UV, visible and infrared radiation and may serve as cloud nuclei (Yin et al., 2002). Additionally, they can have an impact on atmospheric photochemistry by providing a surface for heterogeneous reactions (Schwartz et al., 1995). Thus the presence of dust aerosol alters the surface radiation budget and affects the concentration and distribution of some atmospheric gases like ozone.

*Corresponding author. Tel.: +34 958 244024; fax: +34 958 243214.
E-mail address: alados@ugr.es (L. Alados-Arboledas).

1352-2310/$ - see front matter © 2005 Elsevier Ltd. All rights reserved.
doi:10.1016/j.atmosenv.2005.09.011

The local and global radiative impact of dust aerosol is expected to be larger and more important, relative to the other types of aerosols such as sulphates, due to its large spatial coverage and high load of mineral dust (Haywood et al., 2001; Tanré et al., 2003). The radiative effects of this type of aerosol have received considerable attention in recent years (Sokolik et al., 2001; Highwood et al., 2003; Tanré et al., 2003). The Intergovernmental Panel on Climate Change (2001) suggests a radiative forcing of mineral dust ranging from $-0.6\,W\,m^{-2}$ to $+0.4\,W\,m^{-2}$. However, recent results concerning solar absorption by mineral dust indicate that the global mean radiative forcing is likely negative (Myhre et al., 2003). These last authors have modelled the radiative impact of mineral dust with a comprehensive comparison with measurements obtained during the SHADE campaign. Using the calibrated model they determined a global mean net radiative impact of Saharan dust around $-0.4\,W\,m^{-2}$ when averaged over the globe.

The Sahara desert is one of the principal sources of natural dust in the northern hemisphere. Due to its geographical vicinity with the African continent, our study area is frequently affected by intrusions of Saharan air. Most of these Saharan dust clouds arrive in Spain between May and September (Rodríguez et al., 2001). In the period January–June transport of Saharan dust toward Spain is mainly due to the cyclonic activities over the West or South of Portugal, while in the summer this transport s governed by the anticyclonic activities over the East or Southeast of Iberian Peninsula (Rodríguez et al., 2001). The Saharan air outbreaks cover very large area and are usually highly loaded with mineral particles. The arrival of these air masses icreases the aerosol loading and can introduce pronounced changes in the background atmospheric aerosol optical properties.

On the other hand, the frequent occurrence of African dust outbreaks has implications on air pollution regulation strategies, and accounts for the marked difference in the features of the airborne particulates between Southern and Northern Europe (Rodriguez et al., 2001). The African air masses interfere with the monitoring of the anthropogenic fraction of PM10 (particulate matter $<10\,\mu m$) in the Mediterranean countries, and could result in exceeding the forthcoming EU daily limit for PM10 (Rodriguez et al., 2001).

Characterization of mineral aerosol properties in southeastern Spain is possible because to its proximity to the African continent and allows us to study the Saharan dust just entering the European continent before it possibly mixes with anthropogenic emissions in Europe. In this work we used sun photometer observations, in combination with information from TOMS aerosol index and back trajectory data, to analyse the characteristics of the atmospheric aerosols under Saharan dust intrusions that affected southeastern Spain. The measurements were performed in a rural area on the outskirts of a middle size city in southeastern Spain.

2. Experimental site and data

In this study the principal instrument used is an EKO MS-120 sun photometer. This instrument made measurements of the direct Sun irradiances in four spectral channels centred at 368, 500, 675 and 778 nm. The bandwidth of the interference filters employed in this sun photometer is approximately 5 nm. The MS-120 has a full view angle of 2.4° and a slope angle of 0.9°. The spectral accuracy is better than 2 nm. The instrument was calibrated using the Langley method, which was performed under stable atmospheric conditions (Schmid and Wehrli, 1995). The Langley plot performed presented correlation coefficient about 0.99, with standard deviation about 0.003, although in some cases the aerosol optical depth at 500 nm reached values close to 0.04. In any case the differences in the calibration constant retrieved by using normal Langley plots or refined Langley plots, that is considering different air mass for each attenuator, were rather low and implied differences in the computed aerosol optical depths lower than 0.003. This could be used as indicative of stability. Degradation of instrument calibration was monitored by means of a series of Langley calibrations performed regularly throughout the measurement period.

The sun photometer was in operation at the Meteorological Office of Armilla Air Base (37.18°N, 3.58°W, 660 m a.m.s.l.), located on the outskirts of Granada in Southeastern Spain since 1994–1998 (Alados-Arboledas et al., 2003; Lyamani et al., 2004). The measurements were performed on a daily basis at 09.00, 12.00 and 15.00 GMT on clear days. Measurements on cloudy days were made when clouds were at a significant distance from the solar disc. The synoptic observation programme at the meteorological station was used to guarantee results that were not influenced by cirrus clouds. The sun photometer measurements were performed manually

by experienced staff of the meteorological office. On the other hand, previous to their analyses the data have been revised and checked against the routine information on cloud cover registered in the meteorological office that includes a Celiometer.

3. Methodology

3.1. Aerosol optical depth and Angström turbidity coefficients

The aerosol optical depth, δ_a, is derived from the total optical depth, δ, obtained from sun photometer data using the appropriate calibration constant, obtained by Langley calibrations, and subtracting the Rayleigh optical depth, δ_R, as well as the O_3 and NO_2 absorption optical depths, δ_3 and δ_2 (Alados-Arboledas et al., 2003).

The ozone optical depth was computed using measurements of total ozone columnar concentration at the Global Ozone Observing System station 213, located at El Arenosillo (37.1°N, 6.7°E, 17 m a.m.s.l.). For NO_2 we have used a fixed value of 0.0017 cm atm, which represents an average value for areas influenced by urban emissions (Schroeder and Davies, 1987) and was confirmed by surface measurements of NO_2 at Granada city centre (INM, 1998).

Considering the error sources in derived aerosol optical depths, the uncertainty in the $\delta_a(\lambda)$ is dependent on the wavelength and is lower than 0.02 (Alados-Arboledas et al., 2003).

The Angström turbidity coefficients ($\delta_{a\lambda} = \beta\lambda^{-\alpha}$) has been determined by means of the least-squares fits of the spectral aerosol optical depth (in a log–log scale) in the wavelength range 368–778 nm. The α parameter characterizes the spectral features of aerosols and is related to the size of the particles (Shifrin, 1995). Thus, low values of α, close to 0, are indicative of predominance of large particles in the micrometric range while large values above 1.5 are indicative of predominance of small particles in the submicron range. The β parameter is related to particle concentration and represents the AOD at 1 μm.

3.2. Aerosol size distribution

The aerosol size distribution has been retrieved from the aerosol optical depth using the inversion method of King et al. (1978). The spectral aerosol optical depth is related to the columnar particle size distribution through the scattering equation:

$$\delta_a(\lambda) = \int_{r_a}^{r_b} \pi r^2 \, Q_{ext}(r, \lambda, m) \, n_c(r) \, dr, \quad (1)$$

where Q_{ext} is the Mie extinction efficiency parameter which is a function of the particle radius r, wavelength λ and the complex refractive index m, and $n_c(r)$ is the columnar size distribution. The lower and upper limits of the integration, r_a and r_b, respecively, are defined considering particle sizes that contribute significantly to the integrand in Eq. (1). Therefore, the values of radius interval limits, r_a and r_b, depend on the extreme values of λ used in estimating aerosol optical depths, $\delta_a(\lambda)$.

Limitations of the inversion procedure include the accuracy with which the measurement wavelength is known and number and range of wavelengths over which $\delta_a(\lambda)$ is measured (Amato et al., 1995). Various studies (King et al., 1978; González and Ogren, 1996) point out that the inversions are not substantialy affected by sensitivity to radius limits and refractive index values assumed in the inversions. Following the suggestions made by González and Ogren (1996) and according to criteria defined by Heintzenberg et al. (1981), and also by considering the quoted range of values of refractive index that correspond to different types of aerosol particles (Hess et al., 1998), we have estimated that the independent information content on optical characteristics of columnar aerosols is contained primarily in the particle radius interval from 0.06 to 2 μm for aerosol optical depth measurements covering the spectral range 368–778 nm (Alados-Arboledas et al., 2003).

4. Detection of Saharan dust events

Intrusions of Saharan air masses into the study area can produce an important increase in atmospheric turbidity (high aerosol optical depth values) because these Saharan air masses are highly loaded with mineral particles. Thus, in order to detect Saharan dust events we selected events of high turbidity in which the aerosol optical depth at 500 nm was greater than 0.3. In an attempt to determine their natural or anthropogenic origin, we calculated the corresponding air back trajectories for these cases. Back trajectory data were combined with information obtained from the evaluation of TOMS aerosol index maps. Finally we selected for subsequent analysis those cases with back trajectories showing a Saharan origin of the air masses.

Air back trajectories were computed by means of hybrid sail-particle Lagrangian integrated trajectory (HYSPLIT) model (Draxler and Hess, 1997), using meteorological data supplied by the US National Climatic Center. In each case, a 168-h back trajectory has been calculated for heights of 1500 and 3000 m.

To follow the evolution of Saharan dust events we also used TOMS images from the Earth-Probe satellite. Using channels with very little dependence on ozone the aerosol index is estimated (Herman et al., 1997). The aerosol index (AI) is an indicator of aerosols loading in the study area. Positive values of this index correspond to ultraviolet absorbing aerosol, while negative values correspond to non-absorbing aerosol. Although this index only represents an estimate of aerosol loading in the atmospheric column, it can serve to identify the Saharan dust events (Hsu et al., 1999).

5. Back trajectories analysis

As significant cases of Saharan dust events we analyse those that occurred from 30 August 1998 to 2 September 1998 and on 10 September 1998. The back trajectories for consecutive days around the first and the second event were computed by the HYSPLIT model. For the first event we observed that the back trajectories (Fig. 1a) showed Saharan dust just coming into the study area from North Africa on 30 August. The back trajectories for 3 September showed that all air masses arriving to the study area came from the Atlantic, bringing about the end of the first Saharan dust event. The back trajectories for 10 September (Fig. 1b) indicate an air mass arriving in the study area from North Africa. The second event had very short duration, ending by 11 September when the air masses came from the Atlantic.

6. Aerosol optical depth during the events

The two Saharan dust episodes are characterized by pronounced changes in the aerosol properties usually observed in our area (Fig. 2). As we observe in Fig. 2, the two episodes coincide with marked increase in aerosol optical depth at all wavelengths. In the absence of Saharan dust the value of $\delta_a(500)$ was about 0.2, following the arrival of Saharan air mass the aerosol optical depth at 500 nm increased up to 0.6 in the first event, and up to 0.55 in the second. At the end of the events the arrival of an air

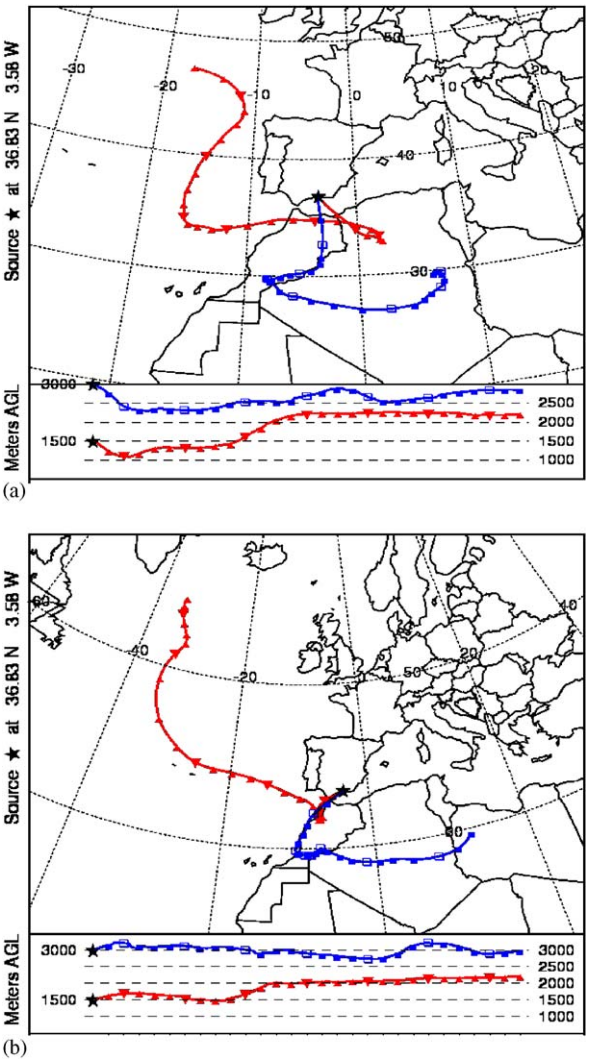

Fig. 1. (a) Back trajectories for 30 August, at 3000 m (squares) and at 1500 m (triangles), finishing at Armilla at 12 UTC. (b) Back trajectories for 10th September 1998, at 3000 m (squares) and at 1500 m (triangles), finishing at Armilla at 12 UTC.

mass from the Atlantic induced a sharp decrease in $\delta_a(500)$ that reached values close to those obtained before each event (~0.2). We can observe good temporal agreement between the results obtained by back trajectory analyses and the aerosol optical depth. Also we observe that during the two Saharan dust episodes the increase in aerosol optical depth were greater at large wavelengths. This could be associated with an increase in the large size particle component. Comparing the two Saharan dust events we observed that the second had a short duration (1 day) and more abrupt effect on aerosol optical depth.

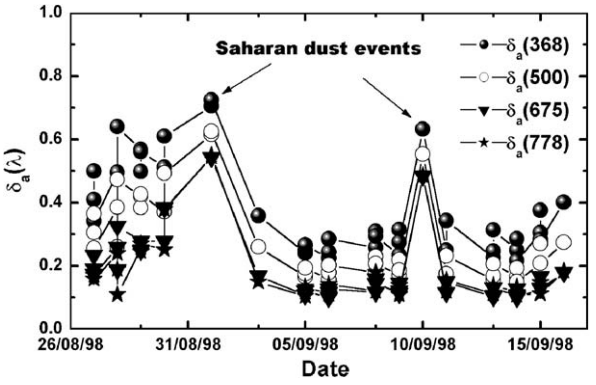

Fig. 2. Temporal evolution of the aerosol optical depth at 368, 500, 675 and 778 nm during the period 26 August 1998–16 September 1998.

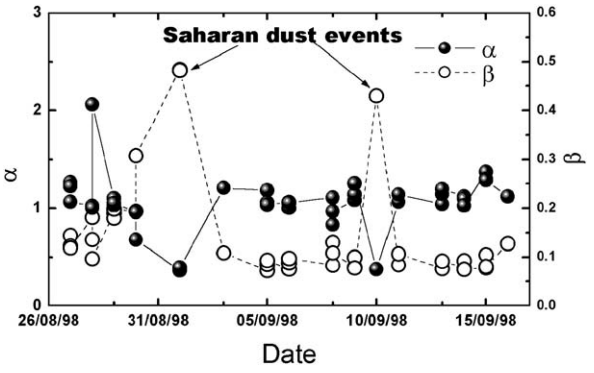

Fig. 3. Temporal evolution of Angström coefficients α and β during the period 26 August 1998–16 September 1998.

Regarding the Angström turbidity coefficients, the arrival of Saharan dust produced a considerable increase in the Angström coefficient β and a drastic decrease in the Angström exponent α, indicating the addition of large particles to the atmospheric column (Fig. 3). During the first Saharan dust episode the Angström exponent α began to decrease on 30 August (when the event began), reached a minimum value of 0.36 on 1 September, and after 3 September (day when the event ended) this parameter approached unity as before the event. During the second Saharan dust episode, the Angström exponent α decreased again and reached a value of 0.37 on 10 September. These minimum values of the Angström exponent α coincided with maximum values of the Angström coefficient β. On the other hand, we observe that the Angström exponent α reached similar values during the two Saharan dust episodes, which indicates that the aerosol particles had similar sizes in both episodes.

During the two Saharan dust episodes the anti-correlation between aerosol optical depth and the Angström exponent α is very evident, indicating that the elevated aerosol concentrations were mainly caused by Saharan dust. Such anti-correlation observed during the Saharan dust episodes was also found by other authors (Kubilay et al., 2003; Smirnov et al., 1998). The aerosol optical depth and the Angström exponent α values for Saharan dust events obtained in this study are in good agreement with those obtained by Smirnov et al. (1998) during the second aerosol characterization experiment (ACE-2). These authors, using AERONET sun photometer data collected on Tenerife, Canary Islands, have reported values of $\delta_a(500)$ ranging from 0.20 to 0.41 and values of Angström exponent α in the range 0.14–0.65 during Saharan dust episodes. Also there is good agreement between the data obtained in this study and the data obtained on other AERONET sites influenced by desert dust (Holben et al., 1998). On the other hand, dust optical depth and Angström exponent α obtained in this work agree well with mean data $\delta_a(500) = 0.61$ and $\alpha = 0.38$ (collected at Gosan, Korea) obtained during Asian Pacific Regional Aerosol Characterization Experiment (ACE-Asia) (Kim et al., 2005). Angstrom exponent spanning the 0.1–0.9 and −0.1–0.7 range have been obtained at Solar-Ville, Saudi Arabia, and Cape Verde, respectively, from AERONET sun photometer measurement to characterize desert dust (Dubovik et al., 2002). As we can conclude, there is good agreement between our results and the results reported by these authors.

In order to explain the tendencies observed in aerosol optical depths and the Angström exponent α, and to follow the evolution of the Saharan air masses that invaded the study area from 30 August until 2 September 1998, we have analysed the images of TOMS aerosol index corresponding to six days around 1 September 1998. These analyses showed that the Saharan air mass that affected the study area on 30 August–2 September was centred over Mauritania on 29 August. On 30 August this Saharan air mass approached Southeastern Spain, and subsequently dispersed over the whole Iberian Peninsula on 31 August and 1 September, producing an important increase in aerosol optical depths and a considerable decrease in the Angström exponent α. The images of TOMS aerosol index corresponding to 3 September do not show any absorbing aerosols over the study area, indicating

the end of this Saharan dust event. These results are in good agreement with those obtained from the analysis of the back trajectories and aerosol optical depth. Concerning the second event, the analyses of images of TOMS aerosol index showed that the Saharan air mass, which affected the study area on 10 September, was centred over the Algerian desert on 9 September. On 10 September the Saharan dust cloud entered the south of the Peninsula, producing an important increase in aerosol optical depths (Fig. 2). By 11 September the Saharan air mass displaced eastward, indicating the end of the event.

7. Aerosol columnar size distributions during the events

Let us now examine the effect of these two Saharan dust events on the aerosol size distributions and other aerosol physical properties. The columnar aerosol size distributions were retrieved from aerosol optical depth measurements using the method of King et al. (1978). The complex refractive indices of particulate matter were selected in a two-step procedure. First, we obtained the real part of the refractive index by trial and error method under the assumption of zero imaginary part. Real refractive indices in the ranges 1.45–1.60 were used (Hänel, 1994). The selected value of the real part of the refractive index was that one which gave the lowest root mean square deviation between calculated and measured $\delta_a(\lambda)$. The retrieved values are about 1.55 for Saharan dust cases, similar to the one used in other studies (Díaz et al., 2000; Patterson et al., 1977), while for non Saharan dust cases the retrieved values are about 1.48, a value confirmed in other studies in rather close locations in the Iberian Peninsula (Vitale et al., 2000). For the imaginary part we have used a value 0.005 that seems appropriate for both kinds of cases (Díaz et al., 2000; Patterson et al., 1977; Vitale et al., 2000). In Fig. 4 we compare the aerosol size distributions retrieved during the Saharan dust episodes with those retrieved for not affected by Saharan dust. The change in the aerosol particle size distributions, shown in the Fig. 4, is evident. The aerosol size distributions corresponding to the days of the Saharan dust episodes were bimodal with a well-defined mode centred at a radius of 0.6 μm, and an evident increase in particle concentration in the size range 0.4–2 μm. Fig. 4 shows that the concentration of particles in the size range 0.4–2 μm corresponding to Saharan dust days was eight times

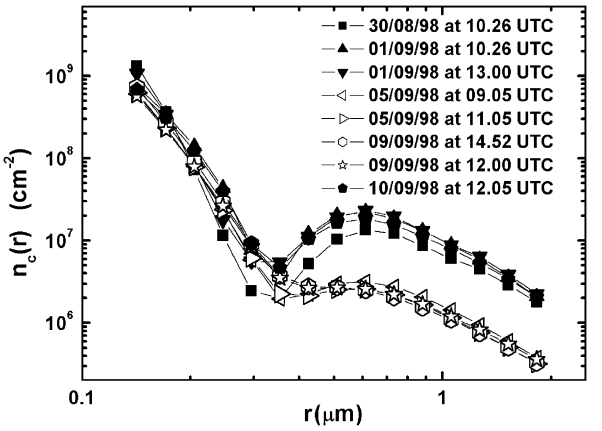

Fig. 4. Aerosol size distributions retrieved during (filled symbols) and in absence (non-filled symbols) of Saharan dust.

greater than that corresponding to days outside of the event. These results are similar to those obtained by Alpert and Ganor (2001). These authors showed, by means of analysis carried out with a scanning electron microscope, that during the Saharan dust event that in Israel in March 1998, a majority of the particles were in the radius range 0.5–2.5 μm. On the other hand, Rodriguez et al. (2001), using the measurements of PM10 from the Andalusian Air Quality Network, identify the same Saharan dust episodes in Granada with PM10 daily values five times greater than those corresponding to the days outside of the first event, reaching daily values of 120 $\mu g\,m^{-3}$ during the episodes peak.

Following a similar procedure used by Alados-Arboledas et al. (2003), we have computed the columnar concentration of small particles N_s ($0.06 < r < 0.35\,\mu m$) and large particles N_l ($0.35 < r < 2\,\mu m$) and evaluated the ratio N_l/N_s. In Fig. 5 we show the variations of N_s, N_l and N_l/N_s during the period 27 August 1998–16 September 1998.

The concentration of small particles during the two events do not present any marked change and it is similar to those observed on days without the effects of Saharan dust. At Jungfraujoch in the Swiss Alps, using a different technique, Schwikowski et al. (1995) showed that the concentration of small particles in the range radius 0.05–0.3 μm do not present any change during the Saharan dust event that occurred on March 1990. On the other hand, we can observe the important increase in the concentration of small particles on 28 August. The back trajectory analyses corresponding to this day show that this increase is associated with the air

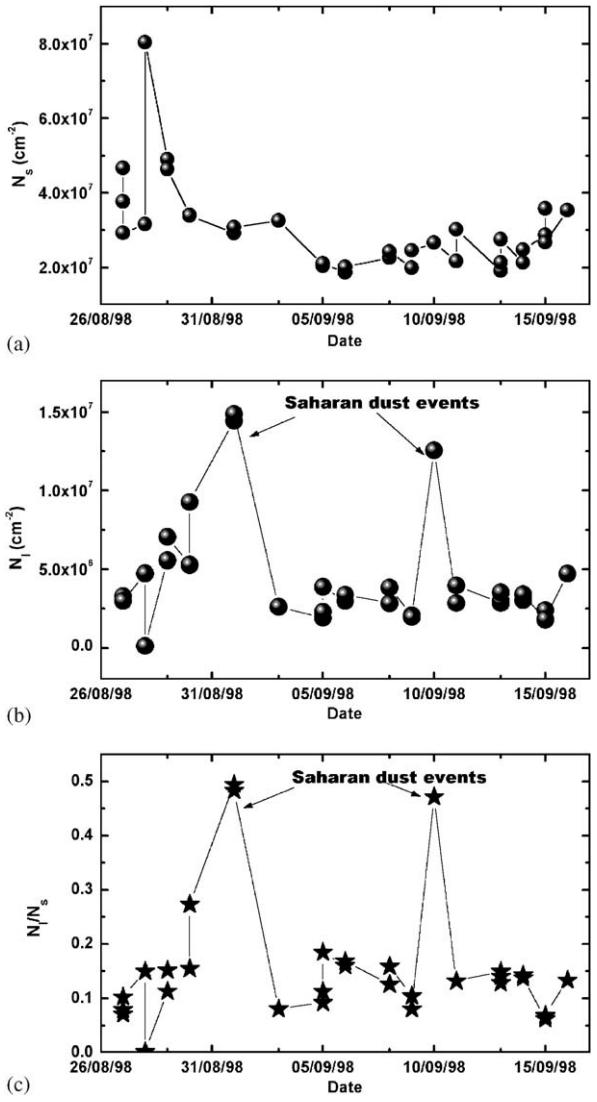

Fig. 5. Temporal variation of: (a) small particle concentration N_s ($0.06<r<0.35\,\mu m$), (b) large particle concentration N_l ($0.35<r<2\,\mu m$), (c) ratio N_l/N_s during the period 26 August 1998–16 September 1998.

mass coming from the Atlantic and passing over areas in southern Spain, where the contamination can be important.

The concentration of large particles presents a drastic increase during the two Saharan dust episodes. This increase is more abrupt and of shorter duration in the second event. The Fig. 5c shows the prevalence of large particles during these two events. These results are similar to those obtained by other authors at different locations (Schwikowski et al., 1995; Afeti and Resch, 2000).

8. Conclusions

Within the context of a project to measure total optical depth from 1994 to 1998 with an EKO sun photometer at the Meteorological Office of Armilla Air Base located in the outskirts of Granada, Spain (37.18°N, 3.58°W, 660 m a.m.s.l.), we have presented a detailed characterization ophysical properties of Saharan dust outbreaks observed over southern Spain, which occurred from 30 August to 3 September 1998 and on 10 September 1998. The effects of these dust events on the region were further confirmed by air mass back trajectory and TOMS aerosol index maps, both of which indicated that the dust-laden air masses effectively originated over the Sahara region.

We showed that large changes occurred in the aerosol properties when Saharan dust outbreaks affect the site. In addition to a marked increase in aerosol optical depth, the Saharan dust outbreaks were characterized by sharp decreases in the Angström exponent indicative of the increase in the large particle mode. The aerosol optical depth and Angström exponent values for Saharan dust periods obtained in our study agree with those obtained ACE-2 and ACE-Asia experiments, as well as with results obtained on certain AERONET sites. During dust episodes, the concentration of large particles in the interval radius 0.4–2 μm increased while the concentration of small particle remained unchanged. Saharan dust showed a bimodal size distribution with a well-defined mode centred at a radius of 0.6 μm. The first event was accompanied by an important increase in the concentration of dust at the surface. Thus, PM10 daily concentrations reached values of about $120\,\mu g\,m^{-3}$ and were five times greater than those obtained without the influence of dust outbreaks.

Acknowledgements

This work was supported by CICYT from the Spanish Ministry of Science and Technology through projects No. CGL2004–05984–C07–03 and REN2003–03175. The Spanish Meteorological Service kindly supplied the sun photometer data. The ozone columnar contents were provided by INTA. Backward trajectories have been obtained by HYSPLIT4, available at the NOAA site http://www.arl.noaa.gov/ready/hysplit4.html, NOAA Air Resources Laboratory, Silver Spring, MD. We

thank Dr. Kowalski who revised the English translation of the manuscript.

References

Afeti, G.M., Resch, F.J., 2000. Physical characteristics of Saharan dust near the Gulf of Guinea. Atmospheric Environment 34, 1273–1279.

Alados-Arboledas, L., Lyamani, H., Olmo, F.J., 2003. Aerosol size properties at Armilla, Granada (Spain). Quarterly Journal of the Royal Meteorological Society 129 (590), 1395–1413.

Alpert, P., Ganor, E., 2001. Saharan mineral dust measurements from TOMS: comparison to surface observations over the Middle East for the extreme dust storm, March 14–17, 1998. Journal of Geophysical Research 106, 18275–18286.

Amato, U., Esposito, F., Serio, C., Pavese, G., Romano, F., 1995. Inverting high-spectral-resolution aerosol optical depth to determine the size distribution of atmospheric aerosol. Aerosol Science and Technology 23 (4), 591–602.

Díaz, J.P., Exposito, F.J., Torres, C.J., Carreño, V., Redondas, A., 2000. Simulation of mineral dust effects on UV-radiation levels. Journal of Geophysical Research 105, 4979–4991.

Draxler, R.R., Hess, G.D., 1997. Description of the HYSPLIT-4 modelling system, NOAA Technical Memorandum, ERL ARL-224, December, p. 24.

Dubovik, O., Holben, B.N., Eck, T.F., Smirnov, A., Kaufman, Y.J., King, M.D., Tanré, D., Slutsker, I., 2002. Variability of absorption and optical properties of key aerosol types observed in worldwide locations. Journal of the Atmospheric Sciences 59 (3) 590–68.

González, H., Ogren, J.A., 1996. Sensitivity of retrieved aerosol properties to assumptions in the inversions of spectral optical depths. Journal of Atmospheric Science 53, 3669–3685.

Hänel, G., 1994. Optical-properties of atmospheric particles—complete parameter sets obtained through polar photometry and an improved inversion technique. Applied Optics 33 (30), 7187–7199.

Haywood, J.M., Francis, P.N., Glew, M.D., Taylor, J.P., 2001. Optical properties and direct radiative effect of Saharan dust: a case study of two Saharan dust outbreaks using aircraft data. Journal of Geophysical Research 106, 18417–18430.

Heintzenberg, J., Muller, H., Quenzel, H., Thomalla, E., 1981. Information content of optical data with respect to aerosol properties: numerical studies with a randomized minimization—serch—technique inversion algorithm. Applied Optics 20, 1308–1315.

Herman, J.R., Bhartia, P.K., Torres, O., Hsu, C., Seftor, C., Celarier, E., 1997. Global distribution of UV-absorbing aerosols from Nimbus 7/Toms data. Journal of Geophysical Research 102, 16911–16922.

Hess, M., Koepke, P., Schult, I., 1998. Optical-properties of aerosols and clouds—the software package OPAC. Bulletin of the American Meteorological Society 79, 831–884.

Highwood, E.J., Haywood, J.M., Silverstone, M.D., Newman, S.M., Taylor, J.P., 2003. Radiative properties and direct effect of Saharan dust measured by the C-130 aircraft during Saharan Dust Experiment (SHADE): 2. Terrestrial spectrum. Journal of Geophysical Research 108, 8578.

Holben, B.N., Eck, T.F., Slutsker, I., et al., 1998. AERONET—A federated instrument network and data archive for aerosol characterization. Remote Sensing of Environment 66 (1), 1–16.

Hsu, N.C., Herman, J.R., Torres, O., Holben, B.N., Tanre, D., Eck, T.F., Smirnov, A., Chatenet, B., Lavenu, F., 1999. Comparison of the TOMS aerosol index with sun photometer aerosol optical thickness: results and application. Journal of Geophysical Research 104, 6269–6279.

INM, 1998. Calendario Meteorológico 1998. Instituto Nacional de Meteorología, Ministerio de Medio Ambiente, Madrid.

IPCC (Intergovernmental Panel on Climate Change), 2001. The Scientific Basis. In: Contribution of working group I to the third assessment report of the intergovernmental panel on climate change, Cambridge University Press, New York, p. 881.

Kim, S.W., Yoon, S.C., Jefferson, A., Ogren, J.A., Duton, E.G., Won, J.G., Ghim, Y.S., Lee, B.I., Han, J.S., 2005. Aerosol optical, chemical and physical properties at Gosan, Korea during Asian dust and pollution episodes in 2001. Atmospheric Environment 39 (1), 39–50.

King, M.D., Byrne, D.M., Herman, B.M., Reagan, J.A., 1978. Aerosol size distribution obtained by inversion of optical depth measurements. Journal of Atmospheric Science 35, 2153–2167.

Kubilay, N., Cokacar, T., Oguz, T., 2003. Optical properties of mineral dust outbreaks over the north-eastern Mediterranean. Journal of Geophysical Research 108 (D21), 4666.

Lyamani, H., Olmo, F.J., Alados-Arboledas, L., 2004. Long-term chage in aerosol radiative properties at Armilla. Atmospheric Environment 38, 5935–5943.

Myhre, G., Grini, A., Haywood, J.M., Stordal, F., Chatenet, B., Tanre, D., Sundet, J.K., Isaksen, I.S.A., 2003. Modeling the radiative impact of mineral dust during the Saharan Dust Experiment (SHADE) campaign. Journal of Geophysical Research 108, 8579.

Patterson, E.M., Gillette, D., Stockton, B.H., 1977. Complex index of refraction between 300 and 700 nm for Saharan aerosols. Journal of Geophysical Research 82, 3153–3160.

Rodríguez, S., Querol, X., Alastuey, A., Kallos, G., Kakaliagou, O., 2001. Saharan dust contribution to PM10 and TSP levels in Southern and Easter Spain. Atmospheric Environment 35, 2433–2447.

Schmid, B., Wehrli, C., 1995. Comparison of sun photometer calibration by use of the Langley Technique and the standard lamp. Applied Optics 34 (21), 4500.

Schroeder, R., Davies, J.A., 1987. Significance of nitrogen dioxide in estimating aerosol optical depth and size distribution. Atmosphere and Ocean 25, 107–114.

Schwartz, S.E., Arnold, F., Blanchet, J.P., Durke, P.A., Hofmann, D.J., Hoppel, W.A., King, M.D., Lacis, A.A., Nakajima, T., Ogren, J.A., Toon, O.B., Wendisch, M., 1995. Group report: connections between aerosol properties and forcing of climate. In: Heintzenberg, J., Charlson, R.J. (Eds.), Aerosol of Climate. Wiley, New York, pp. 251–280.

Schwikowski, M., Seibert, P., Baltensperger, U., Gaggeler, H.W., 1995. A study of an outstanding Saharan dust event at the high-Alpine site Jungfraujoch, Switzerland. Atmospheric Environment 29, 1829–1842.

Shifrin, K.S., 1995. Simple relationships for the Angström parameter of disperse systems. Applied Optics 34, 4480–4485.

Smirnov, A., Holben, B.N., Slutsker, I., Welton, E.J., Formenti, P., 1998. Optical-properties of Saharan dust during ACE-2. Journal of Geophysical Research 103, 28079–28092.

Sokolik, I.N., Winker, D.M., Bergametti, G., Gillette, D.A., Carmichael, G., Kaufman, Y.J., Gomes, L., Schuetz, L., Penner, J.E., 2001. Introduction to special section: Outstanding problems in quantifying the radiative impacts of mineral dust. Journal of Geophysical Research 106, 18015–18027.

Tanré, D., Haywood, J., Pelon, J., Leon, J.F., Chatenet, B., Formenti, P., Francis, P., Goloub, P., Highwood, E.J., Myhre, G., 2003. Measurement and modeling of the Saharan dust radiative impact: overview of the Saharan Dust Experiment (SHADE). Journal of Geophysical Research 108 (D18), 8574.

Vitale, V., Tomasi, C., Lupi, A., Cacciari, A., Marani, S., 2000. Retrieval of columnar aerosol size distributions and radiative-forcing evaluations from sun photometric measurements taken during the CLEARCOLUMN (ACE 2) experiment. Atmospheric Environment 34, 4095–5105.

Yin, Y., Wurzler, S., Levin, Z., Reisin, T., 2002. Interactions of mineral dust particles and clouds: effects on precipitation and cloud optical properties. Journal of Geophysical Research 107 (D23), 4724–4738.